Investigating Weather Impacts on Network-wide Traffic Flow Relationships

Ramin Saedi [a], Ali Zockaie [b]

[a] *Graduate Research Assistant, Michigan State University*
Email: saediger@msu.edu
[b] *Assistant Professor, Michigan State University*
Email: zockaiea@egr.msu.edu

Keywords: *weather change, traffic flow theory, network fundamental diagram, travel time reliability, traffic hysteresis*

Introduction

Traffic state at the network level can be described by network-wide traffic flow relationships such as network fundamental diagram (NFD) (*1–3*), network travel time reliability (TTR) relation (*4*, *5*), total experienced delay, and characteristics of the hysteresis formed due to the network gridlock (*6*). The evaluation of in-field deployment and experimental analyses indicate that macroscopic traffic flow relationships are affected by changes in network supplies, such as climate change, signal coordination, number of accidents, and changes in the specifications of roadways and intersections (*7*, *8*). This study aims to explore the influence of weather changes on network-wide fundamental diagram and travel time reliability relation through a stochasticity analysis. Moreover, an online traffic state prediction framework is created utilizing particle filter estimation engine.

Methodology

In order to investigate the inclement weather impact on network-wide traffic flow relationships, 86 days actual traffic data of Chicago downtown transportation network are employed. Different relationships between traffic flow macroscopic exponents and weather descriptors such as visibility and precipitation are investigated. Mainly, network fundamental diagram and travel time reliability relations are considered to assess the weather impacts on the network level traffic state. Particle filter method is employed for a real-time traffic state prediction. A particle filter is a recursive, Bayesian state approximator that utilizes discrete particles to estimate the subsequent distribution of a system state.

Network Fundamental Diagram

Network fundamental diagram (NFD) represents the aggregated traffic flow-density relationship at the network level. NFD employment leads to generation of new traffic control schemes that may enhance mobility in transportation networks (*9–15*). Relationship between the network-wide weighted average traffic flow and density is used to define the NFD. These variables are calculated as space-mean weighted averages of the link flows and densities, with link weights equal to product of link length and number of lanes (*2*, *16*).

$$Q = \frac{\sum_{i=1}^{M} n_i l_i q_i}{\sum_{i=1}^{M} n_i l_i} \quad (1)$$

$$K = \frac{\sum_{i=1}^{M} n_i l_i k_i}{\sum_{i=1}^{M} n_i l_i} \quad (2)$$

Here, q and k are the link flow and density, Q and K are the weighted average flow and density values respectively, *M* is the number of links in the network, *n* is the number of lanes in each link, and *l* is the link length. This framework yields ordered pairs of macroscopic flow and density values at 5-minute time intervals that cumulatively form the simulation horizon. These values are plotted to give the NFD.

The heterogeneous spatiotemporal distribution of congestion across real networks often creates scatter and hysteresis in the NFD (*17*). A hysteresis is a clockwise loop (complete or incomplete) in the NFD diagram, which shows the level of system instability during the unloading period. In large-scale networks with high levels of congestion, gridlock is formed (*18*), and the system cannot efficiently recover itself during the unloading phase, which causes the formation of a hysteresis loop in the NFD graph. The area of the hysteresis loop (Eq. 3), therefore, is a good representative of system instability.

$$A_{Hys} = \oint_L Q(k)dk \quad (3)$$

where, A_{Hys} is the area of hysteresis loop in NFD, L is the hysteresis closed curve in NFD, and $Q(k)$ is the average network flow as a function of average network density.

Travel Time Reliability

The distance-weighted standard deviation of travel time per unit of distance is often used as a measure of travel time variability. Network travel time reliability can be characterized by a travel time distribution, with corresponding mean and standard deviation. The first component describes the central tendency and the second shows the dispersion. To control for the impacts of trip distance variations on travel time reliability, the travel time (*t*) needs to be normalized by the trip distance (*d*). So, the travel time per unit of distance (*t'=t/d*) is considered as the travel time measure (*5*). Thus, the distance-weighted mean and standard deviation of the travel time *rate* can be estimated as follows:

$$\mu = \frac{\sum_{i=1}^{M} d_i t_i'}{\sum_{i=1}^{M} d_i} = \frac{\sum_{i=1}^{M} t_i}{\sum_{i=1}^{M} d_i} \quad (4)$$

$$\sigma = \sqrt{\frac{\sum_{i=1}^{M} d_i (t_i' - \mu)^2}{\sum_{i=1}^{M} d_i}} \quad (5)$$

In Eq. (4), μ is the inverse of spatial mean speed (*5*). To construct the relationship between distance-weighted mean and standard deviation of travel time rate, a linear model has been suggested in the literature (*19, 20*):

$$\sigma(t') = p_1 + p_2 \mu(t') \quad (6)$$

where

$\sigma(t')$: standard deviation of the trip time rate t',
$\mu(t')$: mean value of t', and
p_1, p_2: coefficients

Particle Filter Estimation

Particle filter estimation approach consists of a system model that relates the model states to measurements. This approach is suitable for online estimations. State estimation is recursively computed by the particle filter algorithm through the steps of initialization, prediction, and correction. Here, the first order difference equation is considered as a state transition function for particle filter algorithm:

$$n(\tau) = n(\tau - 1) + T\left(q(\tau - 1) - G\big(n(\tau - 1)\big)\right) \tag{7}$$

where, the exit function of G(n) is approximated by a third-degree polynomial function of accumulation:

$$\begin{aligned} G\big(n(\tau)\big) &= \alpha_1 n(\tau) + \alpha_2 n^2(\tau) + \alpha_3 n^3(\tau) + WAF(\tau)n(\tau) \\ &= \big(\alpha_1 + WAF(\tau)\big)n(\tau) + \alpha_2 n^2(\tau) + \alpha_3 n^3(\tau) \end{aligned} \tag{8}$$

where
$n(\tau)$: accumulation at time τ,
T: time period of the model,
$q(\tau)$: exogenous traffic flow demand,
$WAF(\tau)$: weather adjustment factor, and
$\alpha_1, \alpha_2, \alpha_3$: coefficients

The particle filter algorithm determines the state estimates of the nonlinear system (traffic flow relationships) using the specified state transition (Eq. 7) and measurement likelihood functions.

Results

DYNASMART-P traffic assignment tool is utilized to simulate the traffic flow in the network using the actual traffic data inputs. Figure 1 illustrates the study area network besides the loading demand profile. Results revealed the existence of robust correlations between the weather index and traffic state describing factors such as coefficient of reliability relation, heterogeneity of density distribution throughout the network, maximum of experienced network-wide average flow and density and the area restricted by hysteresis loop in NFD. Figure 2 illustrates a linear relationship between the spatiotemporal standard deviation of density and the area of hysteresis loop in NFD. According to Figure 3, by increasing the precipitation rate, the throughput is dropped, maximum experienced congestion by the network is increased and the area of hysteresis loop gets larger. An interesting observation is that by intensifying the precipitation rate, network becomes more reliable. One possible reason for this observation is the reduced speed variations, which is the case due to lower adopted speeds by travelers under the harsh weather conditions. Thus, travel time fluctuation is decreased during the high precipitation of snow or rain, and this results in more reliable system.

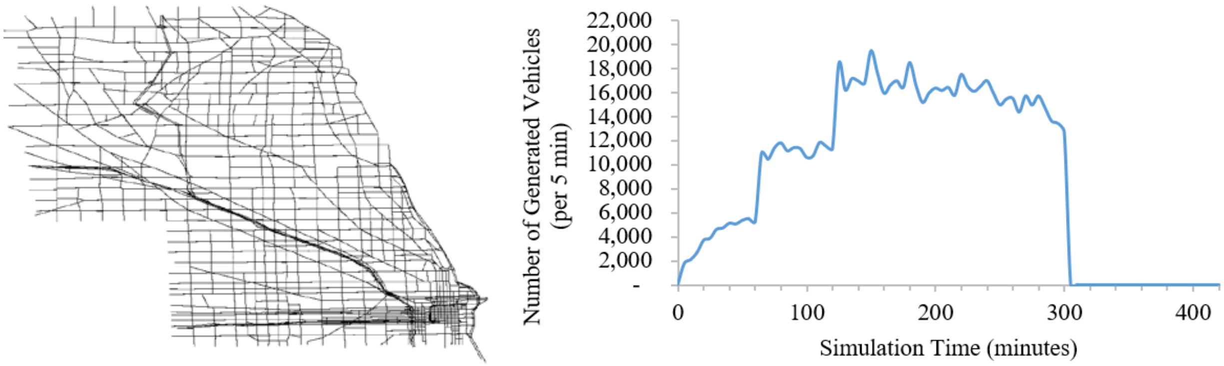

(a) (b)

Figure 1 - (a) study area and (b) loading demand profile

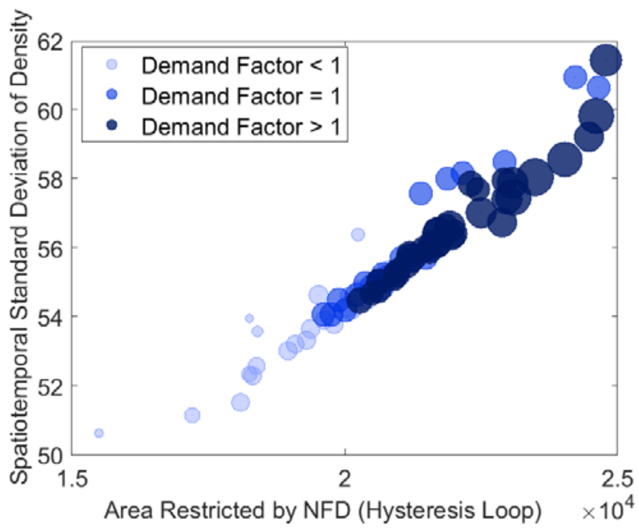

Figure 2 - Relationship between the spatiotemporal standard deviation of density and area of hysteresis loop in NFD graph

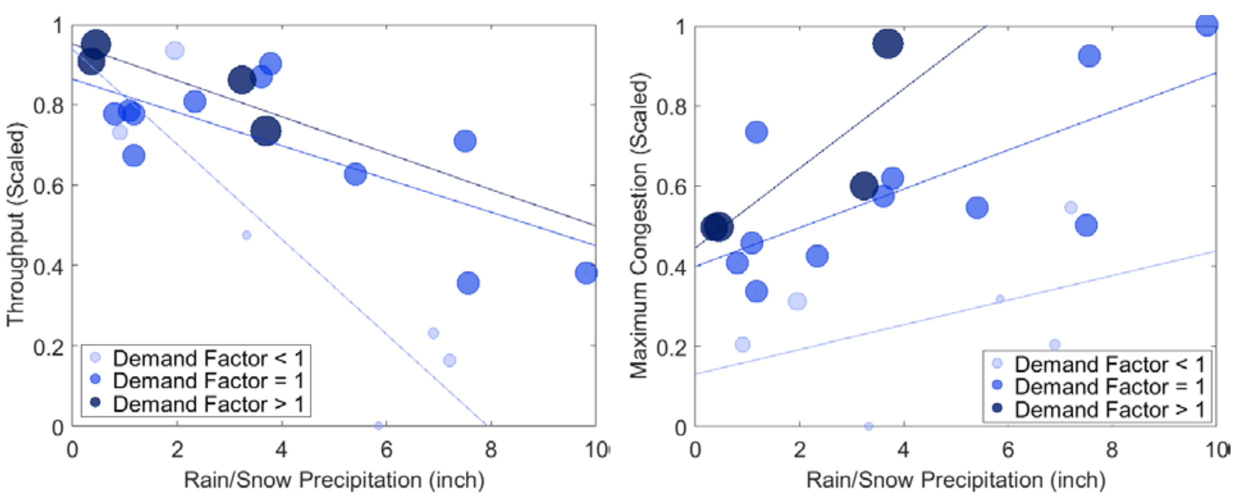

(a) (b)

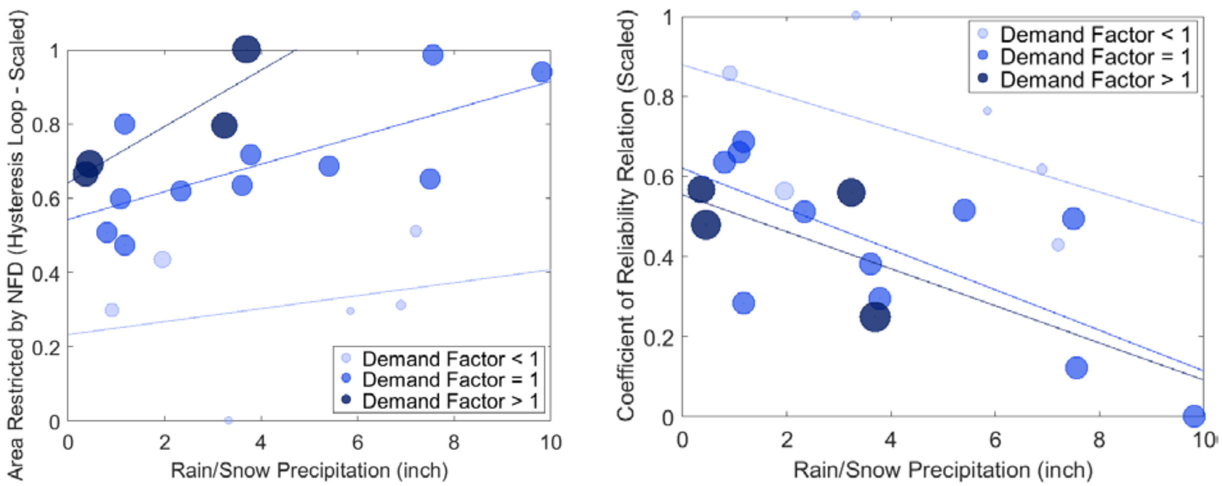

(c) (d)

Figure 3 - Relationship between the rain/snow precipitation rate and (a) network throughput, (b) maximum congestion experienced by the network, (c) hysteresis loop in NFD, and (d) coefficient of reliability relation

Conclusion

Assessing the impacts of inclement weather is accomplished by evaluating the changes in NFD and TTR relations. Traffic data of 86 days of Chicago downtown network is employed to create scenarios with different specifications of demand, weather impact, and number of network-wide incidents. Results discovered a relationship between the precipitation rate and the network-wide traffic state representative factors. A real-time traffic state prediction engine is also created utilizing the particle filter method. Application of this model is examined for Chicago network and a successful calibration and validation process is illustrated. Findings of this research implies the necessity of incorporating a weather factor in network control strategies, demand management and traffic estimation and prediction systems.

References

1. Godfrey, J. W. The Mechanism of a Road Network. *Traffic Engineering & Control*, Vol. 8, No. 8, 1969.
2. Mahmassani, H. S., J. C. Williams, and R. Herman. Investigation of Network-Level Traffic Flow Relationships: Some Simulation Results. *Transportation Research Record*, Vol. 971, 1984, pp. 121–130.
3. Geroliminis, N., and C. F. Daganzo. Existence of Urban-Scale Macroscopic Fundamental Diagrams: Some Experimental Findings. *Transportation Research Part B: Methodological*, Vol. 42, No. 9, 2008, pp. 759–770.
4. Mahmassani, H. S., T. Hou, and J. Dong. Characterizing Travel Time Variability in Vehicular Traffic Networks: Deriving a Robust Relation for Reliability Analysis.

Transportation Research Record, Vol. 2315, No. 1, 2012, pp. 141–152.
5. Mahmassani, H. S., T. Hou, and M. Saberi. Connecting Networkwide Travel Time Reliability and the Network Fundamental Diagram of Traffic Flow. *Transportation Research Record*, Vol. 2391, No. 1, 2013, pp. 80–91.
6. Mahmassani, H. S., M. Saberi, and A. Zockaie. Urban Network Gridlock: Theory, Characteristics, and Dynamics. *Transportation Research Part C: Emerging Technologies*, Vol. 36, 2013, pp. 480–497. https://doi.org/10.1016/j.trc.2013.07.002.
7. Ji, Y., W. Daamen, S. Hoogendoorn, S. Hoogendoorn-Lanser, and X. Qian. Investigating the Shape of the Macroscopic Fundamental Diagram Using Simulation Data. *Transportation Research Record: Journal of the Transportation Research Board*, Vol. 2161, 2010, pp. 40–48. https://doi.org/10.3141/2161-05.
8. Hou, T., H. S. Mahmassani, R. M. Alfelor, J. Kim, and M. Saberi. Calibration of Traffic Flow Models under Adverse Weather and Application in Mesoscopic Network Simulation. *Transportation Research Record*, Vol. 2391, No. 1, 2013, pp. 92–104.
9. Ramezani, M., J. Haddad, and N. Geroliminis. Dynamics of Heterogeneity in Urban Networks: Aggregated Traffic Modeling and Hierarchical Control. *Transportation Research Part B: Methodological*, Vol. 74, 2015, pp. 1–19.
10. Yildirimoglu, M., M. Ramezani, and N. Geroliminis. Equilibrium Analysis and Route Guidance in Large-Scale Networks with MFD Dynamics. *Transportation Research Procedia*, Vol. 9, 2015, pp. 185–204.
11. Haddad, J., and B. Mirkin. Adaptive Perimeter Traffic Control of Urban Road Networks Based on MFD Model with Time Delays. *International Journal of Robust and Nonlinear Control*, Vol. 26, No. 6, 2016, pp. 1267–1285.
12. Mariotte, G., L. Leclercq, and J. A. Laval. Macroscopic Urban Dynamics: Analytical and Numerical Comparisons of Existing Models. *Transportation Research Part B: Methodological*, Vol. 101, 2017, pp. 245–267.
13. Yang, K., N. Zheng, and M. Menendez. Multi-Scale Perimeter Control Approach in a Connected-Vehicle Environment. *Transportation research procedia*, Vol. 23, 2017, pp. 101–120.
14. Zhong, R. X., C. Chen, Y. P. Huang, A. Sumalee, W. H. K. Lam, and D. B. Xu. Robust Perimeter Control for Two Urban Regions with Macroscopic Fundamental Diagrams: A Control-Lyapunov Function Approach. *Transportation Research Part B: Methodological*, 2017.
15. Saedi, R., M. Saeedmanesh, A. Zockaie, M. Saberi, N. Geroliminis, and H. S. Mahmassani. Improving Network Travel Time Reliability Estimation with Network Partitioning. 2018.
16. Saberi, M., H. Mahmassani, T. Hou, and A. Zockaie. Estimating Network Fundamental Diagram Using Three-Dimensional Vehicle Trajectories: Extending Edie's Definitions of Traffic Flow Variables to Networks. *Transportation Research Record: Journal of the Transportation Research Board*, No. 2422, 2014, pp. 12–20.
17. Geroliminis, N., and J. Sun. Properties of a Well-Defined Macroscopic Fundamental Diagram for Urban Traffic. *Transportation Research Part B: Methodological*, Vol. 45, No. 3, 2011, pp. 605–617.
18. Mahmassani, H. S., and M. Saberi. Urban Network Gridlock: Theory, Characteristics, and Dynamics. *Procedia-Social and Behavioral Sciences*, Vol. 80, 2013, pp. 79–98.
19. Richardson, A. J., and M. A. P. Taylor. Travel Time Variability on Commuter Journeys.

High Speed Ground Transportation Journal, Vol. 12, No. 1, 1978.
20. Jones, E. G. Travel Time Variability in a Commuting Corridor : Implications for Electronic Route Guidance. 1989.